Synthesis, structural, vibrational and DFT investigation of new binuclear molecular Pd-Cu and Cu-Cu complexes formed by Schiff base and hexafluoroacetylacetonate building blocks

Evgeniia S. Vikulova[a], Nataliya S. Nikolaeva[a*], Pavel O. Krasnov[b,c],Alexander A. Sukhikh[a,d], Anton I. Smolentsev[a,d], Evgenia A. Kovaleva[b], Natalya B. Morozova[a], Tamara V. Basova[a]

[a] Nikolaev Institute of Inorganic Chemistry SB RAS, Novosibirsk, 630090, Russia
[b] Siberian Federal University, Krasnoyarsk, 660041, Russia
[c] Reshetnev Siberian State University of Science and Technology, Krasnoyarsk, 660049, Russia
[d] Novosibirsk State University, Novosibirsk, 630090, Russia
**corresponding author, e-mail: nikolaeva@niic.nsc.ru*

Abstract

In this work, the first binuclear molecular noble metal-contained complex from the Schiff base (SB) and β-diketonate building blocks, *viz.* [Pd(acacen)Cu(hfac)$_2$], has been synthesized and investigated in comparison with the homometallic binuclear analog [Cu(acacen)Cu(hfac)$_2$]. A detailed comparative characterization of the structure of these new compounds as well as their molecular SB components [M(acacen)] was performed through crystallography, vibrational spectroscopy and DFT calculations. The experimental IR bands have been assigned on the basis of DFT calculations. The Hirshfeld surface analysis was used as a tool for better insight into intermolecular contacts. It has been shown that despite both bimetallic complexes have similar molecular structure and packing style, the nature of the closest intermolecular contacts in [M(acacen)Cu(hfac)$_2$] differs considerably. A topological analysis of the electron density distribution in [M(acacen)] and [M(acacen)Cu(hfac)$_2$] complexes was carried out and the most probable paths of bond cleavage upon decomposition of the compounds were revealed. The binding energies of the molecular components in binuclear complexes were also calculated.

***Keywords**:* bimetallic complexes; palladium (II) complexes; copper (II) complexes; crystal structure; DFT calculations; IR spectra

1. Introduction

1D and 2D nanomaterials of Pd-Cu bimetallic system are widely used in different industrial processes. For example, $Pd_xCu_{(1-x)}$ nanoparticles are utilized as catalysts for CO_2, nitrite and nitrate hydrogenation [1,2], while palladium-containing thin films are one of the most effective membranes for the high purity hydrogen production [3,4]. Chemical vapor deposition methods, particularly, metal-organic chemical vapor deposition (MOCVD) are used for making multicomponent materials with specified properties [5]. However, in addition to common requirements (high volatility, thermal stability, "thermal window" between the vapor sublimation and its decomposition) MOCVD precursors used for these purposes should possess specified physicochemical properties such as compatible deposition temperatures and comprise identical ligands to prevent their exchange in the gas phase. Recently the idea of bimetallic single-source precursors has attracted attention because their application enables to avoid the selection of precursor combinations, to simplify the experimental procedure and to control the gas phase composition.

While chemistry of heteropolynuclear complexes is widely covered in the literature, the data on molecular compounds suitable as precursors in MOCVD processes are very sporadic [6]. Different synthetic procedures based on alkoxides [7–9], carboxylates [10,11], glyoximates [12] etc. have already been described in the literature. In particular, with regard to Pd–Cu volatile compounds, there was no information about bimetallic palladium-containing complexes with ligands of these types due to their insufficient thermal stability until 2014. Indeed, the first bimetallic Pd-Cu precursor was formed due to specific intermolecular interactions of functionalized metal β-diketonates [13–15]. However, such intermolecular interactions were weak and the compounds mostly had polymer structure. In addition, dissociation of such heterometallic compounds could occur on heating. Thus, the design of bimetallic molecular Pd-Cu compounds of a new type is of current importance.

One of the promising approaches is coordination of one metal atom in a complex containing a Schiff's tetradentate base (SB) or similar ligand to another metal atom in the β-diketonate environment. For instance, the pioneer work was devoted to the synthesis and crystal structure of $[Cu(salen)Cu(hfac)_2]$ ($salen^{2-}$ – N,N'-ethylenebis(salicylidenaminato), $hfac^-$ – hexafluoroacetylacetonato) [16]. Later syntheses, crystal structures, and magnetic characterizations of a number of $[M(SB)Ln(\beta\text{-diket})_3]$ (M – Ni, Cu) compounds were reported by Gleizes, Rayzanov, Kuzmina and coworkers [17–20] and the obtained results were mainly presented in the light of comparison of the structural features and magnetic properties of those bimetallic complexes. In the case of $[Ni(SB)La(\beta\text{-diket})_3]$, thermal behavior has been studied and some principles of changes in the thermodynamic and thermal stability in dependence on their crystal structures have been formulated

[17]. That work [14] represented the most comprehensive research in thermochemistry of such compounds. Thus, the attractiveness of this synthetic approach lies in the possibility to manage the thermal properties of the complexes through the varying the nature of SB or β-diketonate components in the bimetallic molecule. The ranges of variation in the volatility of individual palladium and copper chelates with SB or β-diketonate ligands demonstrated in literature [21–24] create a promising base for obtaining effective precursors of this type.

In this work, we combine the Schiff base and β-diketonate building blocks for the first time to prepare a heterobimetallic Pd-Cu compound. For this purpose, [Pd(acacen)] (acacen^{2-} – N,N'-(ethylene)-*bis*(acetylacetoneiminato-) was chosen as an initial SB molecular component because unlike the above mentioned [M(salen)] it does not tend to π-π or M-π stacking interactions. Copper (II) hexafluoroacetylacetonate, [Cu(hfac)$_2$], was used as a β-diketonate component since it exhibits high ability to coordinate donor molecules to copper center due to the presence of electron-withdrawing groups in the ligands [25,26]. Herein, we focus on the study of the structure of the bimetallic heteronuclear complex [Pd(acacen)Cu(hfac)$_2$] in comparison with its homonuclear analogue [Cu(acacen)Cu(hfac)$_2$]. Both new compounds as well as the corresponding mononuclear components were characterized by the methods of elemental analysis, single-crystal X-ray diffractometry and vibrational spectroscopy. The DFT calculations were employed for topological analysis of the electron density distribution and for evaluation of the binding energies of the complex binuclear molecules.

2. Experimental and computational details

2.1. Chemicals and methods

All the chemicals were of analytical reagent grade and used without additional purification. The elemental analysis was carried out using Carlo-Erba 1106 analyzer. IR-spectra of the complexes in KBr and polyethylene pellets were recorded on a Vertex 80 FTIR spectrometer. NMR spectra were recorded on an Avance 500 spectrometer at 500 MHz for ^{1}H NMR and 125 MHz for ^{13}C NMR in $CDCl_3$ solution. The melting points (*m.p.*) were determined by visual method on the Koffler's table.

2.2. Syntheses and characterization

H_2acacen was synthesized by the previously described method [27] through the condensation of ethylenediamine (0.67 mL, 10 mmol) with acetylacetone (2.04 mL, 20 mmol) with subsequent recrystallizations from hexane. Yield: 1.35 g (60%). *m.p.* 110°C. Anal. calc. for $C_{12}H_{20}N_2O_2$: C, 64.3; H, 9.0; N, 12.5. Found: C, 64.0; H, 9.1; N, 12.5.

[Pd(acacen)]. $PdCl_2$ (0.80 g, palladium content 59.845%, 4.5 mmol) was dissolved in 90 mL of acetonitrile upon heating to ~50°C and then the solution of H_2acacen (1.00 g, 4.5 mmol) in 30 mL acetonitrile was added. After stirring during 10 min the solution was mixed with the equimolar amount of KOH (0.51 g, 9.1 mmol) dissolved in minimum amount of water and kept for 10 min. Then water was added in the ratio of 5:1 (vol.). Finally, the product was filtered and purified by double sublimation in vacuum (P = $5\cdot10^{-2}$ Torr, T = 170 – 200°C). Yield: 0.92 g (62%) *m.p.* 226°C. Anal. Calc. for $C_{12}H_{18}N_2O_2Pd$: C, 43.9; H, 5.5; N, 8.5. Found: C, 44.1; H, 5.7; N 8.3. ^{1}H NMR ($CDCl_3$): 1.93 s (6H, $2CH_3$), 1.98 s (6H, $2CH_3$), 3.39 s (4H, $2CH_2$), 4.83 s (2H, CH). ^{13}C NMR ($CDCl_3$): 20.64 (CH_3), 25.37 (CH_3), 55.89 (NCH_2), 99.01 (CH), 161.81 (C=N), 177.51 (C=O).

Cu(II) complexes. [Cu(acacen)] and [Cu(hfac)$_2$] were synthesized according to the method described in the literature [28] by interaction of H_2acacen (1.00 g, 4.5 mmol) or Hhfac (1.28 ml, 9.0 mmol) with as-precipitated $Cu(OH)_2$ (0.50 g, 5.1 mmol, 13% excess) in the presence of acetone (15 mL). $Cu(OH)_2$ was obtained by mixing aqueous solutions of $CuCl_2$(0.68 g, 5.1 mmol) and KOH(0.58 g, 10.3 mmol). After acetone had been evaporated, Cu (II) complexes were extracted by chloroform and purified by double vacuum sublimation.

[Cu(acacen]). Sublimation parameters: T = 110 – 120°C, P = $5\cdot10^{-2}$Torr. Yield: 1.09 g (85%). *m.p.*136-138°C. Anal. Calc. for $C_{12}H_{18}N_2O_2Cu$: C, 50.5; H, 6.4; N, 9.8. Found: C, 50.7; H, 6.3; N, 9.7.

[Cu(hfac)$_2$].Sublimation parameters: T = 60 – 70°C, P = $5\cdot10^{-2}$Torr. Yield: 1.38 g (64 %). *m.p.* 131-132°C. Anal. Calc. for $C_{10}H_2F_{12}O_4Cu$: C, 25.2; H,0.4; F, 47.8. Found: C, 25.3; H, 0.3; F, 47.8.

[M(acacen)Cu(hfac)$_2$], (M = Pd, Cu). Both bimetallic complexes were obtained based on the procedure described in the literature [18]. The chloroform solution (20 mL) of [Pd(acacen)] (0.40 g, 1.2 mmol) or [Cu(acacen)] (0.35 g, 1.2 mmol) was slowly added to chloroform solution (20 mL) of [Cu(hfac)$_2$] (0.58 g, 1.2 mmol) and the mixture was refluxed for 1 hour. The brown crystals of complexes were grown during solvent evaporation. The yield was close to 100%.

[Pd(acacen)Cu(hfac)$_2$]. m.p. 172-174°C. Anal. Calc. for $C_{22}H_{20}N_2F_{12}O_6CuPd$: C, 32.8; H, 3.5; N, 3.5; F, 28.3. Found: C, 32.5; H, 3.4; N, 3.4; F, 28.1.

[Cu(acacen)Cu(hfac)$_2$]. m.p. 177°C. Anal. Calc. for $C_{22}H_{20}N_2F_{12}O_6Cu_2$: C, 34.6; H, 2.6; N, 3.7; F, 29.9. Found: C, 34.2; H, 2.3; N, 3.7; F, 29.6.

2.3. X-ray diffraction studies

Crystals of [Cu(acacen)], [Pd(acacen)] and bimetallic complexes were selected under a microscope and then mounted to the tip of a thin glass fiber with epoxy resin. X-Ray data were collected on a Bruker DUO single-crystal diffractometer (Mo-anode sealed tube with graphite monochromator (λ = 0.71073 Å), APEX II CCD detector), using standard 0.5° frame width φ and ω scans. The frames were collected at 150 K for all compounds except [Cu(acacen)Cu(hfac)$_2$], while for the latter complex the temperature was held at 250K because of crystal splitting during cooling. Apex2 software package (SAINT, SADABS, RLATT) [29] was used for unit cell determination, integration and absorption correction. The obtained *hkl* datasets were processed in Olex2 [30] software, using SHELXT[31] and SHELXL [31] for the structure solution and subsequent refinement. All non-hydrogen atoms were refined anisotropically. ISOR 0.01 0.02 restraints were placed on C8 atom in [Pd(acacen)Cu(hfac)$_2$].

2.4. Computational details

Quantum-chemical calculations of the molecular and electronic structures as well as IR-spectra of [M(acacen)] and [M(acacen)Cu(hfac)$_2$] molecules, where M = Cu, Pd, were carried out by DFT BLYP-D3/def2-SVP method [32–37] with use of the ORCA software package [38,39]. The topological analysis of the electron density distribution functions received as a result of these computations was performed within the scope of Richard Bader “atoms in molecules” theory [40–42] using AIMAll software package (http://aim.tkgristmill.com) for the purpose of identification of the chemical bonds in these compounds along which the cleavage more likely happens.

The geometry optimization of considered compounds was carried out without any symmetry restrictions (e.g. the point group symmetry was C_1). The spin multiplicity in the series of [Cu(acacen)], [Pd(acacen)], [Cu(acacen)Cu(hfac)$_2$] and [Pd(acacen)Cu(hfac)$_2$] molecules was equal to 2, 1, 3 and 2, respectively. The spin states of all molecules were defined with the use of single point calculations of

the structures obtained from the experimental XRD data without their geometries optimization. The energy gaps between these spin states and multiplicities 4, 3, 1 and 4 in this series of molecules are equal to 2.83 eV, 2.62 eV, 0.69 eV and 2.57 eV. It means that all spin states considered in this work are the most energetically favorable (see Fig.S1, Supporting Information for the more details). Therefore, all calculations were performed in the scope of spin unrestricted Kohn-Sham (UKS) theory. Additionally, RI approximation [43–48] was used for IR-spectra calculations.

3. Results and discussion

3.1. Synthesis

New binuclear heteroleptic complexes were synthesized through the co-crystallization of pre-prepared monometallic components [M(acacen)] and [Cu(hfac)$_2$] in the equimolar ratio in chloroform (Scheme 1). Both Pd-Cu and Cu-Cu complexes are formed as brown crystals during evaporation of solvent and stable in air. The compounds can be repeatedly recrystallized from organic solvents such as chloroform and toluene without changing their characteristics (IR spectra, melting points, elemental composition).

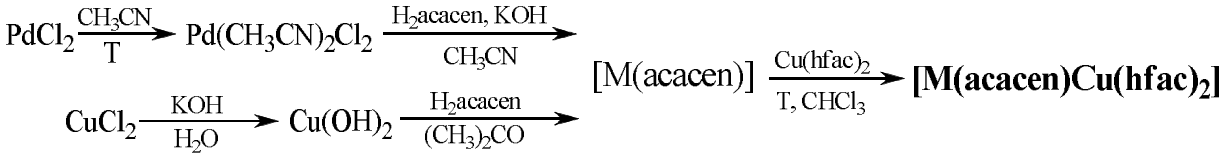

Scheme 1. Synthesis of [M(acacen)Cu(hfac)$_2$] complexes, M = Pd, Cu

3.2. Crystal structures of SB molecular components

To identify the features of the formation of binuclear compounds the individual molecular components were firstly investigated. As for the components of synthesized heteroleptic complexes, only the structure of [Cu(hfac)$_2$] was studied before [49]. The crystal structure of [Cu(acacen)] complex has already been described by Hall *et al.* [50], however the published structure had relatively high R-factor (12%) and no hydrogen atoms were determined. For this reason, the crystal structure of [Cu(acacen)] were refined again using single-crystal X-ray diffraction. The obtained structure is identical to the previously reported [50], but has all hydrogen atoms located with much better R-factor of 2.81%. The crystal structure of [Pd(acacen)] compound has been determined here for the first time. The obtained crystallographic data together with the selected refinement details are given in Table 1.

According to the single-crystal X-ray analysis, [Pd(acacen)] crystallizes in a monoclinic $P2_1/c$ space group with 4 molecules in asymmetric unit. The molecular structure of the complex is shown in Fig.1, while the most relevant bond distances and angles related to the Pd coordination sphere are listed in Table 2. The central Pd atom has nearly square-planar coordination geometry formed by two N and two O donor atoms belonging to the *acacen* ligand. The maximum deviation of Pd atom from the mean N_2O_2 plane is only 0.009 Å. The Pd–O and Pd–N bond lengths as well as bond distances and angles within the ligand are similar to previously reported for related palladium complexes with aliphatic Schiff bases [21,51]. Six-membered metallocycles show no substantial deviation from planarity, making the whole molecule almost planar (maximal deviation from the mean plane is 0.071Å). Methyl groups

are slightly displaced from their "parent" rings; the angle between C–C bridge and the mean plane lies in range from 18.33 to 22.89°.

The unit cell volume of [Pd(acacen)] is 4 times larger compared to that of [Cu(acacen)] with 16 molecules per unit cell. The asymmetric unit contains 4 molecules arranged in two pairs which in turn form alternating parquet layers parallel to the (100) plane (Fig. 1, b). Molecules in pairs are almost parallel (angles between two molecules are equal to 1.83° and 1.94°) and rotated through 180° relative to each other. The distance between two molecules in pairs is ~3.75Å. The angle between two adjacent molecule pairs is 37.36°.

Hirshfeld surface analysis was used for the visualization of intermolecular interactions and identification of close contacts between molecules in the investigated crystals. Fig 2 shows Hirshfeld surfaces [52] generated using Crystal Explorer [53] for [Cu(acacen)] and [Pd(acacen)] complexes, mapped with d_{norm}, curvedness and shape index properties. Since [Pd(acacen)] has 4 individual molecules in unit cell, separate Hirshfeld surfaces were generated for each of them. Surfaces mapped with d_{norm} property with (-0.1÷1.4) scale range show that both complexes have no close contacts between adjacent molecules. Weak red spots mark several C…H, H…H and O…H contacts with interatomic distances between two atoms *ca.*0.1Å smaller than the sum of their Van der Waals radii. At the same time, in the case of [Cu(acacen)] the pairs of red and blue triangles arranged in the form of hourglasses on the surface mapped with the shape index property (Fig. 2, bottom row) indicates π-π interaction between two metallocycles of adjacent [Cu(acacen)] molecules. This π-π interaction also appears as a big flat area on the surface mapped with curvedness property (Fig. 2, middle row). In contrast, no π-π interactions are observed in the case of [Pd(acacen)].

3.3. Crystal structures of binuclear complexes

Molecular structures and packing diagrams of [Cu(acacen)Cu(hfac)$_2$] and [Pd(acacen)Cu(hfac)$_2$] are shown in Fig. 3. The obtained crystallographic data together with the selected refinement details are given in Table 1. The distance between two metal atoms is 3.191Å in [Cu(acacen)Cu(hfac)$_2$] and 3.264Å in [Pd(acacen)Cu(hfac)$_2$].

Bond distances and angles related to the *M(acacen)* fragments are given in Table 2. It should be noted that no significant changes in bond lengths is observed in *M(acacen)* fragment and these molecules retain their flat structure while coordinated. At the same time, N–Cu–O and N–Pd–O angles become bigger, as the *M(acacen)* fragment becomes more elongated towards the Cu atom of Cu(hfac)$_2$. On the

other hand, *Cu(hfac)₂* fragment changes its geometry dramatically (Table 3). The individual complex [Cu(hfac)$_2$] is characterized by a planar geometry [49] with all atoms (except fluorine) deviating from the mean squared plane by no more than 0.08Å, whereas the *Cu(hfac)₂* fragment in the bimetallic complexes is not planar, because coordination of Cu changes from square to octahedral. While *hfac*-ligands remain flat, Cu atoms deviate significantly from the mean planes of both ligands. As a consequence, the bend angles of chelate metallocycle along the line between (OO) donor atoms are equal to 156.13° in [Cu(acacen)Cu(hfac)$_2$] and 162.59° in [Pd(acacen)Cu(hfac)$_2$], whereas in Cu(hfac)$_2$ they are equal to 177.46°. The chelate bond lengths also change significantly. While in individual [Cu(hfac)$_2$] complex they slightly vary from 1.885 to 1.930 Å, in bimetallic [M(acacen)Cu(hfac)$_2$] molecules Cu–O bonds attain the 4+2 configuration: four long Cu–O bonds lie in the plane of M(acacen), and two short Cu–O bonds are perpendicular to the M(acacen) plane. This non-symmetric geometry can be ascribed to the plural ligands with low-symmetric structures. Similar distortions to *Cu(hfac)₂* fragment are also observed in the homobinuclear complex with *salen*-type Schiff base [Cu(salen)Cu(hfac)$_2$] [16], however, in this structure they are noticeably bigger. In particular, the difference between shortest and longest Cu-O bond is 0.35Å and the angle of metallocycle bend along the line between donor atoms can be as low as 149.34°, which is 28° different from the individual [Cu(hfac)$_2$] complex. The other noticeable difference is the lengths of bridge Cu-O bonds between Cu atom of *Cu(hfac)₂* fragment and two oxygen atoms of *M(acacen)*. In both [M(acacen)Cu(hfac)$_2$] complexes these bridge bonds are symmetrically equivalent and equal to 2.179Å for M = Cu and 2.211Å for M = Pd, while in [Cu(salen)Cu(hfac)$_2$] the lengths of these Cu-O bonds are 2.031Å/2.375Å and 1.995Å/2.493Å for two symmetrically independent molecules in the unit cell [16].

Both [Cu(acacen)Cu(hfac)$_2$] and [Pd(acacen)Cu(hfac)$_2$] compounds have columnar packing style along *c* axis (Fig. 3 (b, d)) with M(acacen) parts stacked parallel to each other and facing “inward” the column, while bulky *Cu(hfac)₂* fragments face “outward”. The distance between mean planes of two adjacent *Pd(acacen)* fragments is 3.68 Å, and 3.91 Å between *Cu(acacen)* fragments. Fig. 4 shows Hirshfeld surfaces mapped with the d_{norm} property for [Cu(acacen)Cu(hfac)$_2$] and [Pd(acacen)Cu(hfac)$_2$]. Despite both compounds have the same molecular structure and packing style, the nature of their close intermolecular contacts differs considerably. There are several short (2.85 Å) F…F contacts between *hfac*-ligands in the [Cu(acacen)Cu(hfac)$_2$] complex, while [Pd(acacen)Cu(hfac)$_2$] has weak C–H…O hydrogen bonds (2.5 Å) between neighbor *M(acacen)* fragments.

3.4. Vibrational analysis

The vibrational spectra of the prepared bimetallic complexes were studied and compared with those of their monometallic precursor molecules. The experimental IR and far IR spectra of all complexes are given in Fig. 5. The experimental and calculated IR spectra of [Pd(acacen)] and [Pd(acacen)Cu(hfac)$_2$] are presented in Fig. 6 as an example. The assignment and comparison of the most intense experimental and calculated bands in the IR spectra of complexes are given in Tables S1-S4 (Supporting Information). The experimentally measured vibrational wavenumbers of the molecules coincide well with DFT theoretical predictions. The RMS difference between the calculated and experimental wavenumbers was 20 cm^{-1}.

In the spectra of all derivatives the group of intense bands in the range of 1600-1500 cm^{-1} corresponds mainly to the C=C, C=O, C=N ring stretching vibrations. The bands in two regions of 1445-1354 cm^{-1} and 1040-990 cm^{-1} are mainly attributed to bending vibrations of -CH_3 and -CH_2 groups. The CH out-of-plane vibrations appear as strong bands at 740-760 cm^{-1}. The band with the high contribution of M-O and M-N lies below 700 cm^{-1}. For instance, the most intense bands corresponding to Pd-N and Pd-O stretching vibrations lie at 469, 331, 252 cm^{-1} in the spectrum of [Pd(acacen)], while the bands corresponding to Cu-N and Cu-O are 458 and 362 cm^{-1}. The experimental IR spectrum of [Cu(hfac)$_2$] has already been discussed in the literature [54]. In its spectrum the strong bands in the range 1100–1300 cm^{-1} were mainly assigned to C–F stretching vibrations. Cu–O stretching vibrations mixed with deformations of F-C-C in substituents and ring out-of-plane bending vibrations appeared at ~530 and 325, while the deformations of O-Cu-O and O-Cu-N are observed in the range from 230-260 cm^{-1}. In the IR spectra of bimetallic complexes, the region above 700 cm^{-1} comprises the combination of bands corresponding to the vibrations of both counterparts, whereas bands involving Pd–O, Cu–O stretching and O–Cu–O deformation vibrations in the range from 200 to 700 cm^{-1} are most sensitive to the formation of new Cu–O1 bonds (Fig. 5, Tables S3-S4). For example, the bands at 692, 671, 585, 333, 256, and 235 cm^{-1} in the IR spectrum of [Pd(acacen)Cu(hfac)$_2$] exhibit noticeable shifts (3-5 cm^{-1}) compared to the corresponding bands in spectra of initial [Pd(acacen)] and [Cu(hfac)$_2$] compounds due to the formation of Cu–O1 bond. Two new bands at 492 and 212 cm^{-1} with the high contribution of Cu–O1 stretching and $\delta(OCuO_1)$ vibrations also appear in the [Pd(acacen)Cu(hfac)$_2$] spectrum. Similar shift of several bands at 670, 587, 464, 218, 208 and 218 cm^{-1} and the change of their intensities compared to the spectra of the initial counterparts are observed in the spectrum of [Cu(acacen)Cu(hfac)$_2$]; the new bands at 484 and 292 cm^{-1} appear in the spectra. All these changes indicate the formation of new bonds in bimetallic complexes.

3.5. Topological analysis based on DFT calculations

Both monometallic and bimetallic complexes investigated in this work can be used as CVD precursors for the preparation of metal or metal oxide coatings. For this reason, the knowledge about energy characteristics and other features of intramolecular interactions of individual molecules are very important, for example, for further evaluation of their behavior in the gaseous phase and thermolysis.

Additional insights into the structure of binuclear complexes and their monometallic SB components were obtained through DFT calculations of their individual molecules. The experimental and theoretical geometries of the complexes were shown to be in a good agreement (Tables 2 and 3). The calculated metal-oxygen and metal-nitrogen bond lengths exceed the experimental ones by only 0.04-0.06 Å (Tables 2 and 3), which is less than 2%. The corresponding theoretical valence angles are slightly larger than those determined experimentally, but the difference in the most cases is no more than 1-4º.

As the result of topological analysis of the function of electron density distribution in the [Cu(acacen)] and [Pd(acacen)] complexes, the bond critical points (3,-1) (or BCP) were established and their parameters were estimated (Fig. 7, Table 4). In all cases the interaction between atoms in C-C, C-N and C-O chemical bonds refers to the type of "shared interaction", and bonds themselves refer to covalent type because the values of electron density $\rho(\mathbf{r})$ and its Laplacian $\nabla^2\rho(\mathbf{r})$ in the corresponding critical points are sufficiently high, and the values of $\nabla^2\rho(\mathbf{r})$ are negative (Table S5). The chemical bonds between metal atoms and nitrogen and oxygen atoms are of most interest because the values of their interatomic interaction energy E, estimated as ½ of potential energy density according to the previously published data [55], are the lowest compared to all other chemical bonds (Table 4, Table S5). In the case of M-N bonds, the interaction between these two atoms is of "intermediate" type because of the negative values of $h_e(\mathbf{r})$ in the corresponding critical points. However, the interaction between metal and oxygen atoms refers to the type of "closed-shell interaction" realized through electrostatic attraction, because the values of $\nabla^2\rho(\mathbf{r})$ and $h_e(\mathbf{r})$ are positive. At the same time, the M-O1 and M-O2 atom pairs in the case of both molecules possess the lowest values of interatomic interaction energy; therefore, the cleavage of these bonds is the most probable. The same conclusion was made for a series of the related *bis*-chelated (O^N)-coordinated palladium(II) complexes [56] indicating that the trend to the preferred cleavage of M-O bonds rather than M-N ones may be common for the considered metals in a near square-planar coordination environment.

Topological analysis of the electron density distribution function in the [Cu(acacen)Cu(hfac)$_2$] and [Pd(acacen)Cu(hfac)$_2$] compounds (Fig. 8) shows that the nature of interaction between atom pairs such as carbon-carbon, carbon-nitrogen and carbon-oxygen is identical to that observed in [Cu(acacen)] and [Pd(acacen)] molecules. Similar situation is also observed for M-O1, M-O2, M-N1 и M-N2 bonds (Table S6).

The bridge Cu-O1 and Cu-O2 bonds between both parts in [Cu(acacen)Cu(hfac)$_2$] and [Pd(acacen)Cu(hfac)$_2$] molecules possess the lower values of electron density in the corresponding critical points (3,-1) and, as a consequence, the lower values of interatomic interaction energy (Table 5). For this reason, the cleavage of Cu-O1 and Cu-O2 bonds is most probable.

The detected values of the electron density and its Laplacian at the bond critical points between copper or palladium atoms and oxygen or nitrogen atoms are in good agreement with the results of other works (Tables 4, 5 and S6). For example, it was shown for dipeptide Cu(glygly)$(OH_2)_2$ complex on the basis of topological analysis of experimental data that $\rho(\mathbf{r})$ in the BCPs in the atomic pairs Cu-O and Cu-N is in the range 0.3-0.8 e/Å^3, while $\nabla^2\rho(\mathbf{r})$ has a value from 3 to 13 e/Å^5 [*I. Bytheway, B.N. Figgis, A.N. Sobolev, Charge density in Cu(glygly)(OH$_2$)$_2$·H$_2$O at 10 K and the reproducibility of atomic orbital populations, J. Chem. Soc., Dalton Trans. (2001) 3285-3294. DOI: 10.1039/b102891j*]. In the case of other type of compounds, e.g. Cu$(H_2O)_5$ and Cu$(H_2O)_6$, where copper atom interacts with oxygen atoms of water molecules, the values of electron density and its Laplacian in the corresponding bond critical points lie in the ranges of 0.31-0.57 e/Å^3 and 4.92-12.36 e/Å^5, respectively [*M. Malček, M.N.D.S. Cordeiro, A DFT and QTAIM study of the adsorption of organic molecules over the copper-doped coronene and circumcoronene, Physica E 95 (2018) 59-57. DOI: 10.1016/j.physe.2017.09.004. M. Malček, L. Bučinský, F. Teixeira, M.N.D.S. Cordeiro, Detection of simple inorganic and organic molecules over Cu-decorated circumcoronene: a combined DFT and QTAIM study, Phys. Chem. Chem. Phys. 20 (2018) 16021-16032. DOI: 10.1039/c8cp02035c*]. The values of $\rho(\mathbf{r})$ in the BCPs in the Pd-O and Pd-N atomic pairs of the Pd(II)-salen complex are in the ranges of 0.66-0.73 e/Å^3 and 0.68-0.85 e/Å^3, while the corresponding values of $\nabla^2\rho(\mathbf{r})$ are in the ranges of 12.68-15.04 e/Å^5 and 10.68-13.88 e/Å^5, correspondingly [*M. Azam, S.I. Al-Resayes, S.M. Soliman, A.T. Kruszynska, R. Kruszynski, Synthesis, structural characterization, crystal structure and theoretical study of a Pd(II)-salen complex with propylene linkage, J. Mol. Struct. 1137 (2017) 310-319. DOI: 10.1016/j.molstruc.2017.02.007*].

Six additional bond critical points are also observed in [Cu(acacen)Cu(hfac)$_2$] (Fig. 8). Four of them are between four hydrogen atoms of two CH_3-groups of *Cu(acacen)* and four oxygen atoms of *Cu(hfac)$_2$*, while the other two points are between two hydrogen atoms of two CH_3-groups of *Cu(acacen)* and two fluorine atoms of two CF_3-groups. At the same time, there are only two such points between two hydrogen atoms of two CH_3-groups of *Pd(acacen)* and two oxygen atoms of *Cu(hfac)$_2$* in [Pd(acacen)Cu(hfac)$_2$]. These bond critical points indicate the existence of hydrogen bonds between the mentioned pairs of atoms. The values of $\rho(\mathbf{r})$ and $\nabla^2\rho(\mathbf{r})$ for typical hydrogen bonds is in the range of 0.013-0.236 e/Å^3 and 0.578-3.350 e/Å^5, correspondingly [42].

The sum of energies of interatomic interactions between atoms in the bridge Cu-O bonds is 5.72 eV in the case of [Cu(acacen)Cu(hfac)$_2$] and 5.90 eV in the case of [Pd(acacen)Cu(hfac)$_2$]. However, they increase to 6.18 eV and 6.08 eV, correspondingly, if hydrogen bonds are taken into account. Therefore, the binding between *Cu(hfac)$_2$* and *Cu(acacen)* fragments is stronger than that between *Cu(hfac)$_2$* and *Pd(acacen)*. This fact was also confirmed by the results of calculation of the binding energy between *M(acacen)* and *Cu(hfac)$_2$* fragments in bimetallic compounds according to the equation (1)

$$E_b = E_{M(acacen)} + E_{Cu(hfac)2} - E_{M(acacen)Cu(hfac)2} \quad (1)$$

The binding energy (E_b) was calculated as the difference of the total energies of the corresponding compound and its initial components. It was shown that E_b was equal to 1.64 eV for M = Cu, and 1.44 eV when M = Pd, indicating the higher stability of [Cu(acacen)Cu(hfac)$_2$] in comparison with [Pd(acacen)Cu(hfac)$_2$]. These values are little bit higher compared to the binding energy of 1.31 eV (30.2 kcal/mol) obtained for [Cu(salen)La(ptac)$_3$] (ptac – pivaloyltrifluoroacetonato) [16] (the only data available for such systems). The binding energy values are rather low and indicate that such binuclear complexes may dissociate to monometallic precursors in gas phase upon heating. The experimental investigations of the behavior of bimetallic complexes in gas phase and their application as MOCVD precursors are of great interest and will be a subject of future works. In addition, the binuclear complexes synthesized here can be used to obtain molecular metal-organic films by physical vapor deposition [57,58], and the proximity of metal centers the molecules of this type can exhibit interesting magnetic properties [26,59].

4. Conclusion

In this work, the binuclear [Pd(acacen)Cu(hfac)$_2$] complex has been synthesized and investigated as the first example of heterobimetallic molecular compounds formed by Schiff base and β-diketonate building blocks with noble metals. The detailed characterization of the structure of this compound in comparison with the homometallic binuclear analogue [Cu(acacen)Cu(hfac)$_2$] and the corresponding molecular SB components [M(acacen)] was performed by single crystal X-ray diffraction, vibrational spectroscopy and DFT calculations. It has been shown that the structure of SB complex molecules is almost unchanged after coordination of these molecules to *Cu(hfac)$_2$*. Despite both bimetallic complexes have similar molecular structure and packing style, the nature of the closest intermolecular contacts in [M(acacen)Cu(hfac)$_2$] differs considerably. In particular, Hirshfeld surface analysis reveals several short (2.85 Å) F…F contacts between *hfac*-ligands in the [Cu(acacen)Cu(hfac)$_2$] crystals, while the weak C–H…O hydrogen bonds (2.5 Å) between neighbor *M(acacen)* fragments is found for [Pd(acacen)Cu(hfac)$_2$].

Additional insights into the structure of binuclear complexes and their monometallic SB components were obtained through DFT calculations of their individual molecules.

According to the DFT calculations, a little stronger binding between *M(acacen)* and *Cu(hfac)$_2$* components is observed in the binuclear complexes [Cu(acacen)Cu(hfac)$_2$]. Nevertheless, the demonstrated ability of palladium(II) SB complexes to coordinate to fluorinated β-diketonates with acceptor metal centers opens up a new way for the development of bimetallic Pd-M complexes for various applications. The approach to the preparation of binuclear complexes described in this work shows can be as the starting point for the creation of homo- and heterobimetallic complexes with other 3*d*-transition metals.

Acknowledgements

The authors acknowledge the Russian Foundation for Basic Research for a financial support (project № 18-33-20128) of the part of work associated with the investigation of spectral properties and the Ministry of Science and Education of the Russian Federation for a financial support of the part of work on structural studies of compounds.

References

[1] S. Bai, Q. Shao, P. Wang, Q. Dai, X. Wang, X. Huang, Highly Active and Selective Hydrogenation of CO2 to Ethanol by Ordered Pd–Cu Nanoparticles, J. Am. Chem. Soc. 139 (2017) 6827–6830. doi:10.1021/jacs.7b03101.

[2] T. Ye, D.P. Durkin, N.A. Banek, M.J. Wagner, D. Shuai, Graphitic Carbon Nitride Supported Ultrafine Pd and Pd-Cu Catalysts: Enhanced Reactivity, Selectivity, and Longevity for Nitrite and Nitrate Hydrogenation, ACS Appl. Mater. Interfaces. (2017). doi:10.1021/acsami.7b09192.

[3] N.W. Ockwig, T.M. Nenoff, Membranes for hydrogen separation, Chem. Rev. 107 (2007) 4078–4110. doi:10.1021/cr0501792.

[4] B.H. Howard, R.P. Killmeyer, K.S. Rothenberger, A. V. Cugini, B.D. Morreale, R.M. Enick, et al., Hydrogen permeance of palladium-copper alloy membranes over a wide range of temperatures and pressures, J. Memb. Sci. 241 (2004) 207–218. doi:10.1016/j.memsci.2004.04.031.

[5] A.C. Jones, M.L. Hitchman, Chemical Vapour Deposition, 2008. doi:10.1039/9781847558794.

[6] S. Mishra, S. Daniele, Metal-organic derivatives with fluorinated ligands as precursors for inorganic nanomaterials, Chem. Rev. 115 (2015) 8379–8448. doi:10.1021/cr400637c.

[7] E. Jung, S.H. Yoo, T.M. Chung, C.G. Kim, Y. Kim, D.Y. Jung, Heterobimetallic lithium organoaluminum and organogallium complexes: Potential single precursors for MOCVD of LiMO2thin films, Inorg. Chem. Commun. 5 (2002) 439–441. doi:10.1016/S1387-7003(02)00438-0.

[8] M. Vehkamäki, M. Ritala, M. Leskelä, A.C. Jones, H.O. Davies, T. Sajavaara, et al., Atomic Layer Deposition of Strontium Tantalate Thin Films from Bimetallic Precursors and Water, J. Electrochem. Soc. 151 (2004) F69–F72. doi:10.1149/1.1648025.

[9] P.C. Andrews, P.C. Junk, I. Nuzhnaya, D.T. Thielemann, Bismuth pyrostannate, Bi2Sn2O7, from the first structurally characterized heterobimetallic Bi:Sn alkoxides, Inorg. Chem. 51 (2012) 751–753. doi:10.1021/ic202707p.

[10] T.C. Deivaraj, J.H. Park, M. Afzaal, P. O'Brien, J.J. Vittal, Novel bimetallic thiocarboxylate compounds as single-source precursors to binary and ternary metal sulfide materials, Chem. Mater. 15 (2003) 2383–2391. doi:10.1021/cm031027v.

[11] B. Li, H. Zhang, L. Huynh, C. Diverchy, S. Hermans, M. Devillers, et al., Bismuth-palladium heterometallic carboxylate as a single-source precursor for the carbon-supported Pd-Bi/C catalysts, Inorg. Chem. 48 (2009) 6152–6158. doi:10.1021/ic900505v.

[12] B. Fraser, L. Brandt, W.K. Stovall, H.D. Kaesz, S.I. Khan, F. Maury, Investigation of [(py) (Et) Co(dmg*GaEt2)2] and [Ni(dmg*GaEt2)2] (py = pyridine; dmg = dimethylglyoximato) as single source precursors for deposition of β-CoGa and NiGa by MOCVD. Crystal structure of [(py)(Et)Co(dmg*GaEt2)(dmgH)], J. Organomet. Chem. 472 (1994) 317–328. doi:10.1016/0022-328X(94)80218-1.

[13] V. V. Krisyuk, I.A. Baidina, A.E. Turgambaeva, V.A. Nadolinny, S.G. Kozlova, I. V. Korolkov, et al., Volatile Heterobimetallic Complexes from Pd II and Cu II β-Diketonates: Structure, Magnetic Anisotropy, and Thermal Properties Related to the Chemical Vapor Deposition of CuPd Thin Films, Chempluschem. 80 (2015) 1457–1464. doi:10.1002/cplu.201500050.

[14] V. V Krisyuk, S. V Sysoev, A.E. Turgambaeva, A.A. Nazarova, T.P. Koretskaya, I.K. Igumenov, et al., Thermal behavior of methoxy-substituted Pd and Cu β-diketonates and their heterobimetallic complex, J. Therm. Anal. Calorim. 130 (2017) 1105–1110. doi:10.1007/s10973-017-6469-z.

[15] V. V Krisyuk, Y. V Shubin, F. Senocq, A.E. Turgambaeva, T. Duguet, I.K. Igumenov, et al., Chemical vapor deposition of Pd/Cu alloy films from a new single source precursor, J. Cryst. Growth. (2014) 1–5. doi:10.1016/j.jcrysgro.2014.09.032.

[16] N. Bresciani-Pahor, M. Calligaris, G. Nardin, L. Randaccio, The X-Ray Crystal Structure of Bis(1,1,1,5,5,5-hexafluoropentane-2,4- dionato)copper(II)-N,N'-ethylenebis(salicylideneaminato)copper(II), Transit. Met. Chem. 5 (1980) 180–183. doi:https://doi.org/10.1007/BF01396906.

[17] N.P. Kuzmina, I.P. Malkerova, A.S. Alikhanyan, A.N. Gleizes, The use of 3d-metal complexes as ligands to prepare volatile 4f–3d heterobimetallic complexes, J. Alloys Compd. 374 (2004) 315–319. doi:10.1016/J.JALLCOM.2003.11.098.

[18] A. Gleizes, M. Julve, N. Kuzmina, A. Alikhanyan, F. Lloret, I. Malkerova, et al., Heterobimetallic d-f metal complexes as potential single-source precursors for MOCVD: Structure and thermodynamic study of the sublimation of [Ni(salen)Ln(hfa)(3)], Ln = Y, Gd, Eur. J. Inorg. Chem. (1998) 1169–1174. doi:10.1002/(SICI)1099-0682(199808)1998:8<1169::AID-EJIC1169>3.0.CO;2-Q.

[19] A. Rogachev, N. Kuzmina, A. Nemukhin, Theoretical modeling of the heterobimetallic complex [La(pta)3Cu(salen)] and its precursors, J. Alloys Compd. 374 (2004) 335–338. doi:10.1016/j.jallcom.2003.11.110.

[20] M. Ryazanov, V. Nikiforov, F. Lloret, M. Julve, N. Kuzmina, A. Gleizes, Magnetically isolated CuIIGdIII pairs in the series [Cu(acacen)Gd(pta)3], [Cu(acacen)Gd(hfa)3], [Cu(salen)Gd(pta)3], and [Cu(salen)Gd(hfa)3], Inorg. Chem. 41 (2002) 1816–1823. doi:10.1021/ic0110777.

[21] E.S. Vikulova, S.A. Cherkasov, N.S. Nikolaeva, A.I. Smolentsev, S. V. Sysoev, N.B. Morozova, Thermal behavior of volatile palladium(II) complexes with tetradentate Schiff bases containing propylene-diimine bridge, J. Therm. Anal. Calorim. 135 (2019) 2573–2582. doi:10.1007/s10973-018-7371-z.

[22] S.I. Dorovskikh, N. V Kuratieva, S. V Tkachev, S. V Trubin, P.A. Stabnikov, N.B. Morozova, Copper(II) complexes with Schiff bases: Structures and thermal behavior, J. Struct. Chem. 55 (2014) 1067–1074. doi:10.1134/S0022476614060092.

[23] G.I. Zharkova, P.A. Stabnikov, S.A. Sysoev, I.K. Igumenov, Volatility and Crystal Lattice Energy of Palladium(Ii) Chelates, J. Struct. Chem. 46 (2005) 320–327. doi:10.1007/s10947-006-0047-8.

[24] I.K. Igumenov, T. V Basova, V.R. Belosludov, Volatile Precursors for Films Deposition: Vapor Pressure, Structure and Thermodynamics, in: M. Tadashi (Ed.), Appl. Thermodyn. to Biol. Mater. Sci., IntechOpen, Rijeka, 2011. doi:10.5772/13356.

[25] K.J. de Almeida, T.C. Ramalho, M.C. Alves, O. Vahtras, Theoretical insights into the visible near-infrared absorption spectra of Bis(hexafluoroacetylacetonate) copper(II) in pyridine, Int. J. Quantum Chem. 112 (2012) 2571–2577. doi:10.1002/qua.23273.

[26] M.I. Mocanu, S. Shova, F. Lloret, M. Julve, M. Andruh, Homo- and heterometallic complexes constructed from hexafluoroacetylacetonato and Schiff-base complexes as building-blocks, J. Coord. Chem. 71 (2018) 693–706. doi:10.1080/00958972.2018.1434877.

[27] P.J. McCarthy, R.J. Hovey, K. Ueno, A.E. Martell, Inner Complex Chelates. I. Analogs of Bisacetylacetoneethylenediimine and its Metal Chelates1,2, J. Am. Chem. Soc. 77 (1955) 5820–5824. doi:10.1021/ja01627a011.

[28] I.A. Baidina, P.A. Stabnikov, A.D. Vasiliev, S.A. Gromilov, I.K. Igumenov, Crystal and molecular structure of copper (II) trans-bis-(2-(methylimino)-4-pentanonate), J. Struct. Chem. 45 (2004) 671–677.

[29] Bruker AXS Inc. APEX2 V2013.6-2, SAINT V8.32B and SADABS-2012/1., Bruker Adv. X-Ray Solut. Madison, Wisconsin, USA. (n.d.).

[30] O. V Dolomanov, L.J. Bourhis, R.J. Gildea, J.A.K. Howard, H. Puschmann, OLEX2: a complete

structure solution, refinement and analysis program, J. Appl. Crystallogr. 42 (2009) 339–341. doi:10.1107/S0021889808042726.

[31] G.M. Sheldrick, SHELXT - Integrated space-group and crystal-structure determination, Acta Crystallogr. Sect. A Found. Crystallogr. 71 (2015) 3–8. doi:10.1107/S2053273314026370.

[32] A.D. Becke, Density-functional exchange-energy approximation with correct asymptotic behavior, Phys. Rev. A. 38 (1988) 3098–3100. doi:10.1103/PhysRevA.38.3098.

[33] S. Grimme, S. Ehrlich, L. Goerigk, Effect of the damping function in dispersion corrected density functional theory, J. Comput. Chem. 32 (2011) 1456–1465. doi:10.1002/jcc.21759.

[34] S. Grimme, J. Antony, S. Ehrlich, H. Krieg, A consistent and accurate ab initio parametrization of density functional dispersion correction (DFT-D) for the 94 elements H-Pu, J. Chem. Phys. 132 (2010) 154104. doi:10.1063/1.3382344.

[35] A. Schäfer, H. Horn, R. Ahlrichs, Fully optimized contracted Gaussian basis sets for atoms Li to Kr, J. Chem. Phys. 97 (1992) 2571. doi:10.1063/1.463096.

[36] C. Lee, W. Yang, R.G. Parr, Development of the Colle-Salvetti correlation-energy formula into a functional of the electron density, Phys. Rev. B. 37 (1988) 785–789. doi:10.1103/PhysRevB.37.785.

[37] A. Schäfer, C. Huber, R. Ahlrichs, Fully optimized contracted Gaussian basis sets of triple zeta valence quality for atoms Li to Kr, J. Chem. Phys. 100 (1994) 5829. doi:10.1063/1.467146.

[38] F. Neese, The ORCA program system, Wiley Interdiscip. Rev. Comput. Mol. Sci. 2 (2012) 73–78. doi:10.1002/wcms.81.

[39] F. Neese, Software update: the ORCA program system, version 4.0, Wiley Interdiscip. Rev. Comput. Mol. Sci. 8 (2018) e1327. doi:10.1002/wcms.1327.

[40] R.F.W. Bader, H. Essén, The characterization of atomic interactions, J. Chem. Phys. 80 (1984) 1943. doi:10.1063/1.446956.

[41] R.F.W. Bader, Atoms in Molecules, Acc. Chem. Res. 18 (1985) 9–15. doi:10.1002/prot.10414.

[42] I.S. Bushmarinov, K.A. Lyssenko, M.Y. Antipin, Atomic energy in the “Atoms in Molecules” theory and its use for solving chemical problems, Russ. Chem. Rev. 78 (2009) 283. doi:10.1070/RC2009v078n04ABEH004017.

[43] E.J. Baerends, D.E. Ellis, P. Ros, Self-consistent molecular Hartree-Fock-Slater calculations I. The computational procedure, Chem. Phys. 2 (1973) 41–51. doi:10.1016/0301-0104(73)80059-X.

[44] B.I. Dunlap, J.W.D. Connolly, J.R. Sabin, On some approximations in applications of Xα theory, J. Chem. Phys. 71 (1979) 3396. doi:10.1063/1.438728.

[45] C. Van Alsenoy, Ab initio calculations on large molecules: The multiplicative integral

approximation, J. Comput. Chem. 9 (1988) 620–626. doi:10.1002/jcc.540090607.

[46] A.R. Kendall, A.H. Früchtl, R.A. Kendall, H.A. Früchtl, The impact of the resolution of the identity approximate integral method on modern ab initio algorithm development, Theor. Chem. Acc. 97 (1997) 158–163. doi:10.1007/s002140050249.

[47] K. Eichkorn, O. Treutler, H. Öhm, M. Häser, R. Ahlrichs, Auxiliary basis sets to approximate Coulomb potentials, Chem. Phys. Lett. 242 (1995) 652–660. doi:10.1016/0009-2614(95)00838-U.

[48] K. Eichkorn, F. Weigend, O. Treutler, R. Ahlrichs, Auxiliary basis sets for main row atoms and transition metals and their use to approximate Coulomb potentials, Theor. Chem. Acc. 97 (1997) 119–124. doi:10.1007/s002140050244.

[49] S.A. Gromilov, I.A. Baidina, P.A. Stabnikov, Crystal structure of copper(II) bis-hexafluoroacetylacetonat, J. Struct. Chem. 45 (2004) 502–507.

[50] D. Hall, A.D. Rae, T.N. Waters, The colour, isomerism, and structure of some copper co-ordination compounds. Part V. The crystal structure of NN′-ethylenebis(acetylacetoneiminato)copper(II), J. Chem. Soc. (1963) 5897–5901. doi:10.1039/JR9630005897.

[51] S.A. Cherkasov, E.S. Vikulova, N.S. Nikolaeva, A.I. Smolentsev, N.B. Morozova, Crystal structure and thermal properties of N,N′-(2,2-dimethylpropylene)-bis(acetylacetoneiminato)palladium(II), J. Struct. Chem. 58 (2017) 1453–1456. doi:10.1134/S0022476617070277.

[52] F.L. Hirshfeld, Bonded-atom fragments for describing molecular charge densities, Theor. Chim. Acta. 44 (1977) 129–138. doi:10.1007/BF00549096.

[53] M.J. Turner, J.J. McKinnon, S.K. Wolff, D.J. Grimwood, P.R. Spackman, D. Jayatilaka, et al., CrystalExplorer17, Univ. West. Aust. (2017). http://hirshfeldsurface.net.

[54] M.L. Morris, R.W. Moshier, R.E. Sievers, Infrared Spectra of Metal Chelate Compounds of Hexafluoroacetylacetone, Inorg. Chem. 2 (1963) 411–412. doi:10.1021/ic50006a042.

[55] E. Espinosa, E. Molins, C. Lecomte, Hydrogen bond strengths revealed by topological analyses of experimentally observed electron densities, Chem. Phys. Lett. 285 (1998) 170–173. doi:10.1016/S0009-2614(98)00036-0.

[56] P.O. Krasnov, N.S. Mikhaleva, A.A. Kuzubov, N.S. Nikolaeva, G.I. Zharkova, L.A. Sheludyakova, et al., Prediction of the relative probability and the kinetic parameters of bonds breakage in the molecules of palladium MOCVD precursors, J. Mol. Struct. 1139 (2017) 269–274. doi:10.1016/j.molstruc.2017.03.049.

[57] W. Chen, S. Luo, Z. Wan, X. Feng, X. Liu, Z. He, Ruthenium acetylacetonate in interface

engineering for high performance planar hybrid perovskite solar cells, Opt. Express. 25 (2017) A253–A263. doi:10.1364/oe.25.00a253.

[58] R.K. Sodhi, S. Paul, An Overview of Metal Acetylacetonates: Developing Areas/Routes to New Materials and Applications in Organic Syntheses, Catal. Surv. from Asia. (2018) 31–62. doi:10.1007/s10563-017-9239-9.

[59] M.R. Modaberi, S. Brahma, R. Rooydell, R.-C. Wang, C.-P. Liu, Novel hybrid transition metal complexes of diaquabis(acetylacetonato-κ2o,o′)[nickel(II)/zinc (II)] as solid metal–organic precursors: Synthesis, properties and magnetic response, Appl. Organomet. Chem. 31 (2017) e3746. doi:10.1002/aoc.3746.

Table 1. Crystallographic data and selected refinement details

Compound	[Cu(acacen)]	[Pd(acacen)]	[Cu(acacen)Cu(hfac)$_2$]	[Pd(acacen)Cu(hfac)$_2$]
Formula	$C_{12}H_{18}CuN_2O_2$	$C_{12}H_{18}N_2O_2Pd$	$C_{22}H_{20}Cu_2F_{12}N_2O_6$	$C_{22}H_{20}N_2O_6F_{12}CuPd$
F.W.	285.82	328.68	763.48	806.34
Temperature/K	150	150	250	150
Space group	$P2_1/c$	$P2_1/c$	C2/c	C2/c
a/Å	10.9580(3)	13.6878(6)	18.6599(9)	17.8001(7)
b/Å	8.9714(2)	19.5327(12)	19.2046(11)	18.3194(7)
c/Å	12.8174(3)	21.9344(9)	8.5667(4)	8.6028(3)
β/°	93.4770(10)	119.446(3)	109.706(2)	92.2600(10)
Volume/Å^3	1257.74(5)	5106.8(5)	2890.1(3)	2803.08(18)
Z	4	16	4	4
ρ_{calc} /g·cm^{-3}	1.509	1.710	1.755	1.911
F(000)	596	2656	1520	1588
Reflections/Independent reflections	8446/3115	31659/11422	7592/3612	11663/3501
R_{int}/R_{sigma}	2.33% /3.15%	5.59% / 8.28%	1.87% / 2.95%	2.68% / 2.41%
Data/restraints/parameters	3115/0/158	11422/0/629	3612/0/202	3501/6/202
Goodness-of-fit on F^2	1.032	0.968	1.027	1.079
Final R indexes [I>=2σ (I)] / %	R_1 = 2.81 wR_2 = 6.77	R_1 = 4.57 wR_2 = 7.48	R_1 = 4.89 wR_2 =13.10%	R_1 = 5.08 wR_2 = 12.08
Final R indexes [all data] / %	R_1 = 3.62 wR_2 = 7.10	R_1 = 9.46 wR_2 = 9.17	R_1 = 7.19 wR_2 = 14.90	R_1 = 6.18 wR_2 = 13.21
CCDC№	1961113	1961114	1961115	1961116

Table 2. Bond lengths and angles of *Cu(acacen)* and *Pd(acacen)* fragments as individual complexes and in bimetallic complexes. DFT results are presented as *italic* in brackets.

Parameter	[Cu(acacen)]	*Cu(acacen)* in [Cu(acacen)Cu(hfac)$_2$]	[Pd(acacen)]	*Pd(acacen)* in [Pd(acacen)Cu(hfac)$_2$]
M–O / Å	1.919-1.925 (*1.965-1.966*)	1.925 (*1.967*)	1.997-2.006 (*2.066*)	2.004 (*2.053*)
<M–O> / Å	1.922 (*1.966*)	1.925 (*1.967*)	2.002 (*2.066*)	2.004 (*2.053*)
M–N / Å	1.938-1.941 (*1.981-1.982*)	1.920 (*1.964*)	1.956-1.976 (*2.022-2.023*)	1.953 (*2.006*)
<M–N> / Å	1.940 (*1.982*)	1.920 (*1.964*)	1.965 (*2.023*)	1.953 (*2.006*)
∠N–M–O /°	93.18-93.64 (*93.40-93.47*)	95.14 (*94.21*)	94.55-94.88 (*93.56*)	95.96 (*94.77*)
∠<N–M–O> /°	93.41 (*93.43*)	95.14 (*94.21*)	94.71 (*93.56*)	95.96 (*94.77*)

∠(C–C / "mean plane") /°	21.57 (*21.90*)	15.32 (*21.35*)	18.33-22.89 (*22.27*)	19.58 (*21.86*)

Table 3. Bond lengths and angles for [Cu(hfac)$_2$] molecule and *Cu(hfac)$_2$* fragments in binuclear complexes. DFT results are presented as *italic* in brackets.

Parameter	[Cu(hfac)$_2$] [49]	*Cu(hfac)$_2$* in [Cu(salen)Cu(hfac)$_2$] [16]	*Cu(hfac)$_2$* in [Cu(acacen)Cu(hfac)$_2$] [this work]	*Cu(hfac)$_2$* in [Pd(acacen)Cu(hfac)$_2$] [this work]
Cu–O / Å	1.885-1.930	1.937-2.288	1.934-2.136 (*1.976-2.163*)	1.936-2.114 (*1.962-2.141*)
<Cu–O> / Å	1.912	2.043	2.035 (*2.070*)	2.025 (2.052)
∠O–Cu–O /°	92.20-93.68	86.35-89.06	87.48 (*88.51-90.31*)	90.05 (*89.69-91.62*)
∠<O–Cu–O> /°	92.94	87.71	87.48 (*89.41*)	90.05 (*90.79*)
∠ (metallocycle folding along (O,O) line) / °	177.46	149.34-172.82	156.13° (*158.29°*)	162.59° (*166.66°*)

Table 4. Topological parameters of the $\rho(\mathbf{r})$ function in the critical points (3,-1) of metal-nitrogen and metal-oxygen bonds of M(acacen) molecules

Bond	Cu(acacen)				Pd(acacen)			
	$\rho(\mathbf{r})$, e/Å^3	$\nabla^2\rho(\mathbf{r})$, e/Å^5	$h_e(\mathbf{r})$, au	E, eV	$\rho(\mathbf{r})$, e/Å^3	$\nabla^2\rho(\mathbf{r})$, e/Å^5	$h_e(\mathbf{r})$, au	E, eV
M-N1	0.592	11.39	$-3.84\cdot10^{-3}$	1.71	0.742	11.73	$-1.70\cdot10^{-2}$	2.12
M-N2	0.590	11.35	$-3.77\cdot10^{-3}$	1.70	0.742	11.73	$-1.70\cdot10^{-2}$	2.12
M-O1	0.519	12.56	$8.59\cdot10^{-3}$	1.54	0.568	12.48	$5.69\cdot10^{-3}$	1.61
M-O2	0.519	12.56	$8.59\cdot10^{-3}$	1.54	0.568	12.48	$5.69\cdot10^{-3}$	1.61

Table 5. Topological parameters of the $\rho(\mathbf{r})$ function in the critical points (3,-1) of metal-nitrogen, metal-oxygen and hydrogen bonds of [M(acacen)Cu(hfac)$_2$] molecules

Bond	[Cu(acacen)Cu(hfac)$_2$]				[Pd(acacen)Cu(hfac)$_2$]			
	$\rho(\mathbf{r})$, e/Å^3	$\nabla^2\rho(\mathbf{r})$, e/Å^5	$h_e(\mathbf{r})$, au	E, eV	$\rho(\mathbf{r})$, e/Å^3	$\nabla^2\rho(\mathbf{r})$, e/Å^5	$h_e(\mathbf{r})$, au	E, eV
Cu-O1	0.292	5.13	$2.57\cdot10^{-3}$	0.65	0.268	4.48	$1.57\cdot10^{-3}$	0.59
Cu-O2	0.292	5.13	$2.56\cdot10^{-3}$	0.65	0.268	4.48	$1.57\cdot10^{-3}$	0.59

Cu-O3'	0.341	6.36	$4.01 \cdot 10^{-3}$	0.79	0.358	6.97	$4.75 \cdot 10^{-3}$	0.85
Cu-O3''	0.498	11.79	$9.05 \cdot 10^{-3}$	1.42	0.516	12.41	$8.90 \cdot 10^{-3}$	1.51
Cu-O4'	0.341	6.36	$4.01 \cdot 10^{-3}$	0.79	0.358	6.97	$4.75 \cdot 10^{-3}$	0.85
Cu-O4''	0.498	11.79	$9.05 \cdot 10^{-3}$	1.42	0.516	12.41	$8.90 \cdot 10^{-3}$	1.51
O3'-H	0.076	0.92	$8.23 \cdot 10^{-4}$	0.11	0.065	0.81	$9.03 \cdot 10^{-4}$	0.09
O4'-H	0.076	0.92	$8.23 \cdot 10^{-4}$	0.11	0.065	0.81	$9.03 \cdot 10^{-4}$	0.09
O3''-H	0.042	0.57	$8.92 \cdot 10^{-4}$	0.06	–	–	–	–
O4''-H	0.042	0.57	$8.92 \cdot 10^{-4}$	0.06	–	–	–	–
F-H	0.042	0.59	$8.21 \cdot 10^{-4}$	0.06	–	–	–	–
F-H	0.042	0.59	$8.21 \cdot 10^{-4}$	0.06	–	–	–	–

Figure captions

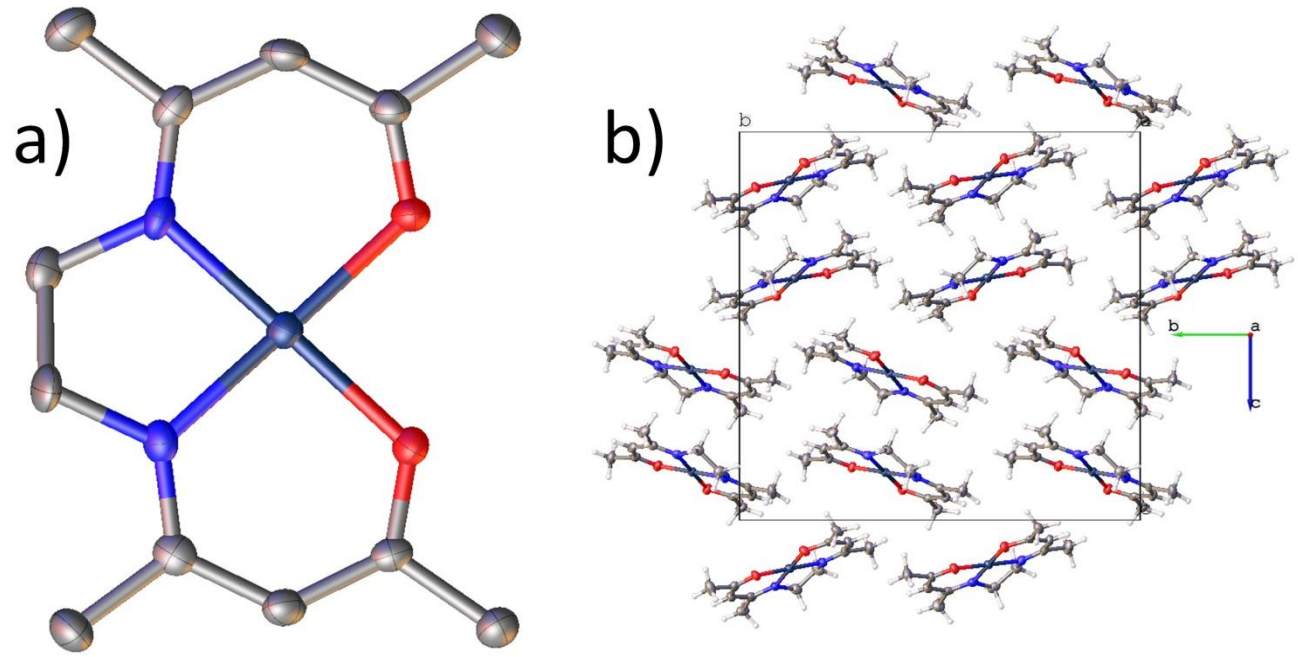

Figure 1. Molecular structure of [Pd(acacen)] complex (a) and packing diagram (b, view along a axis)

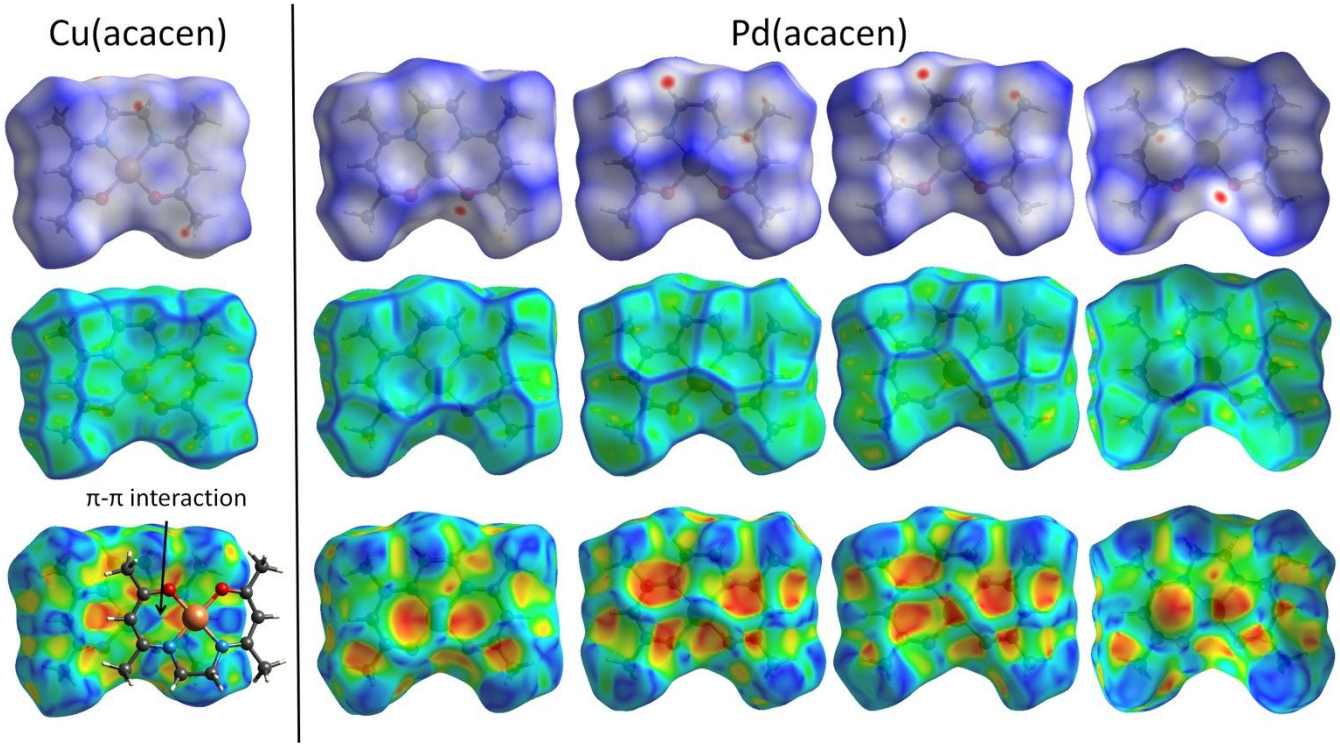

Figure 2. Hirshfeld surfaces for [Cu(acacen)] and [Pd(acacen)] complexes, mapped with d_{norm} (top row), curvedness (middle row) and shape index (bottom row).

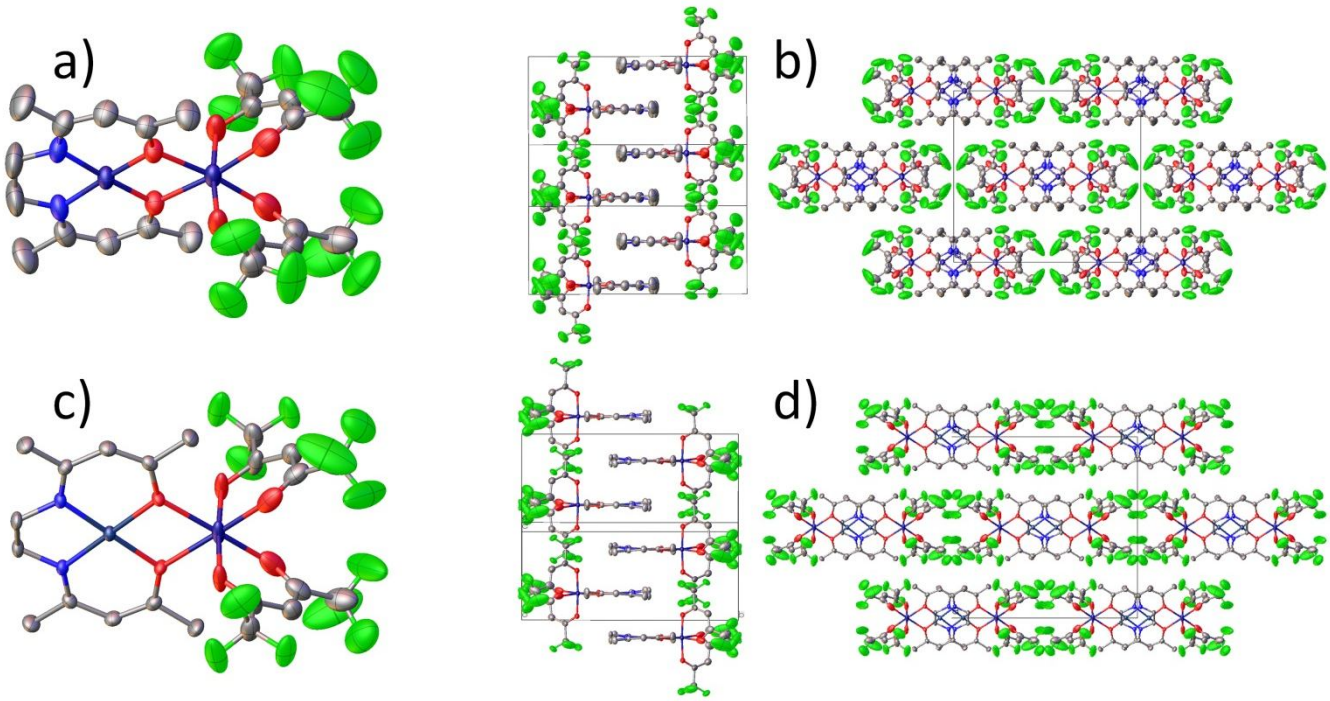

Figure 3. Molecular structure (a) and packing diagram (b) of [Cu(acacen)Cu(hfac)$_2$] complex and molecular structure (c) and packing diagram (d) of [Pd(acacen)Cu(hfac)$_2$].

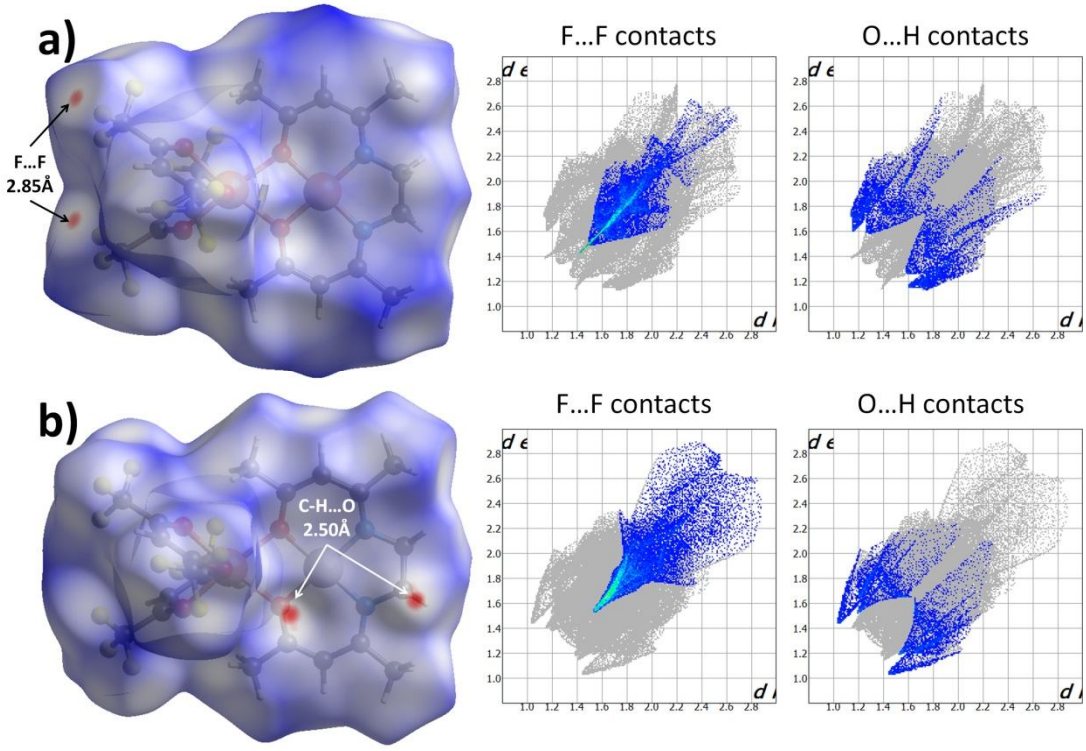

Figure 4. Hirshfeld surfaces mapped with d_{norm} property (-0.1÷1.7 range) and fingerprint plots for [Cu(acacen)Cu(hfac)$_2$] (a) and [Pd(acacen)Cu(hfac)$_2$] (b).

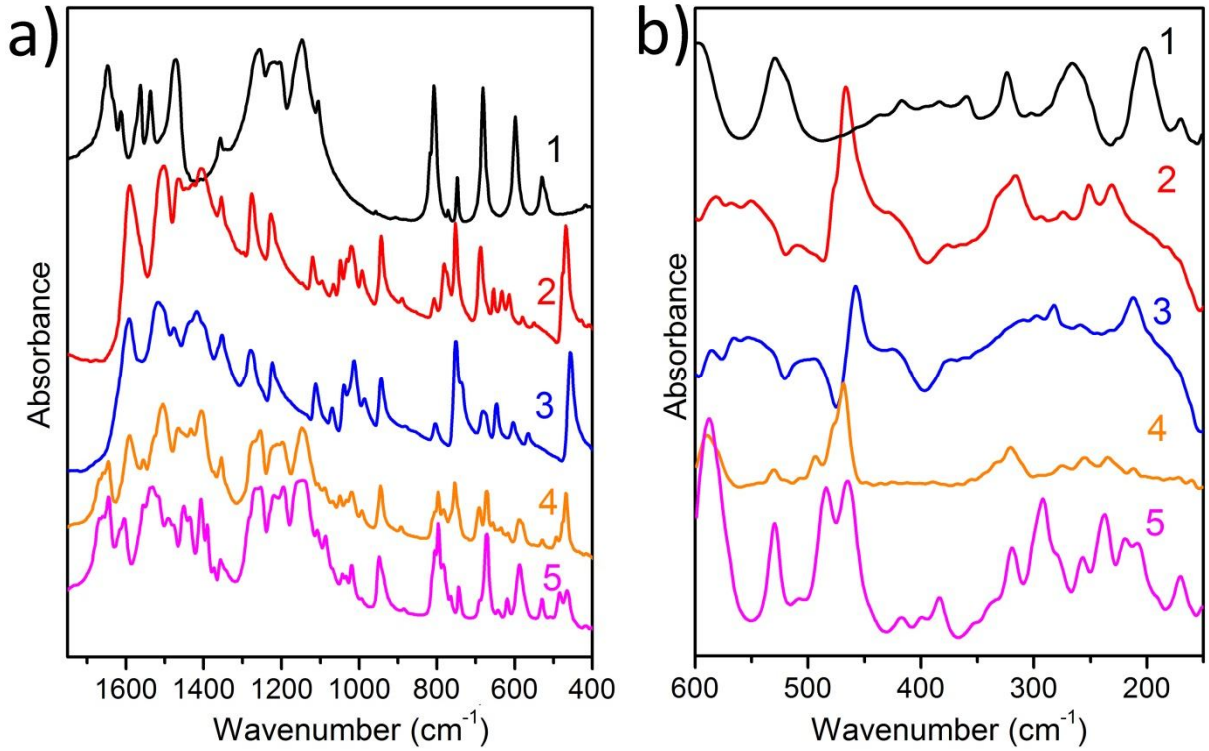

Figure 5. Experimental IR (a) and far IR spectra (b): 1 – $[Cu(hfac)_2]$, 2 – [Pd(acacen)], 3 – [Cu(acacen)], 4 – $[Pd(acacen)Cu(hfac)_2]$, 5 – $[Cu(acacen)Cu(hfac)_2]$.

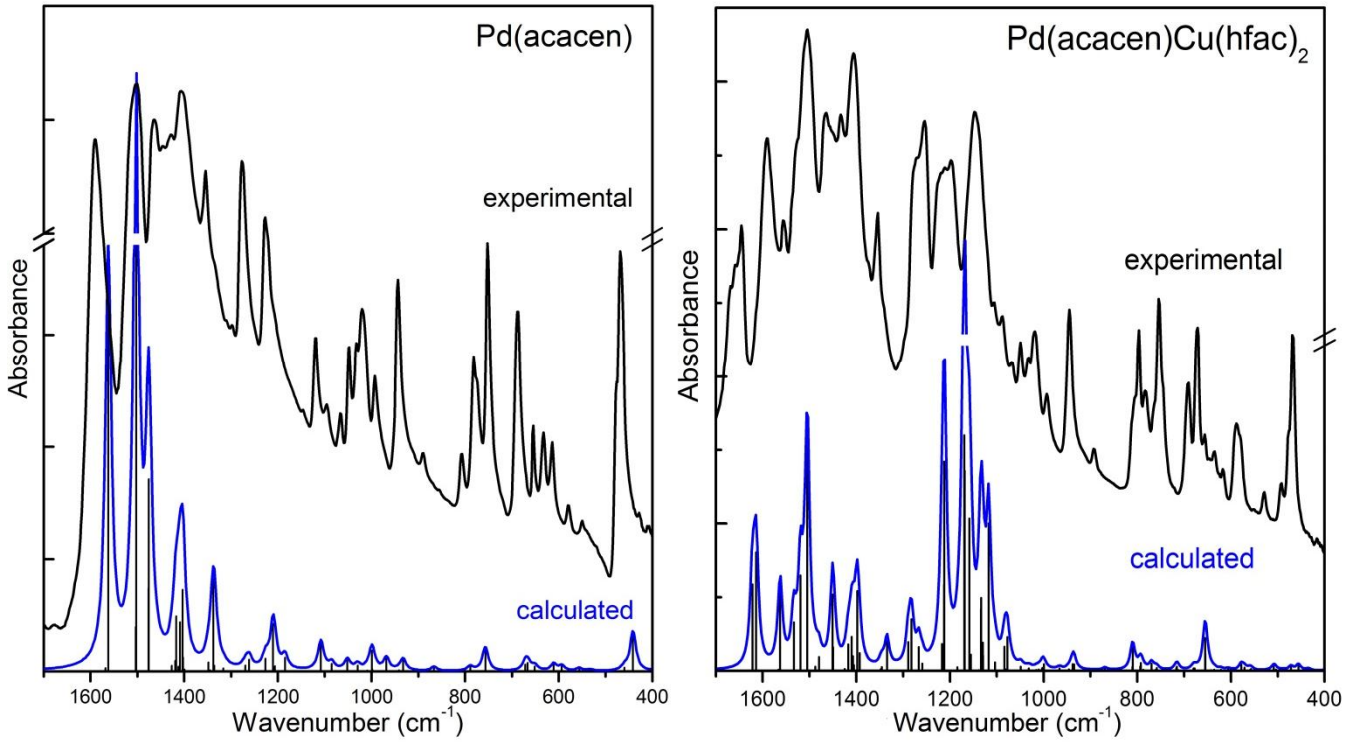

Figure 6. Experimental and calculated IR spectra of [Pd(acacen)] and $[Pd(acacen)Cu(hfac)_2]$.

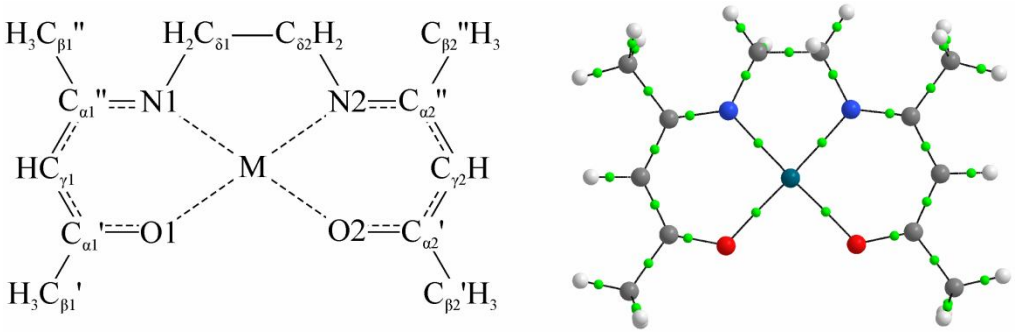

Figure 7. Structural formula of [M(acacen)], where M = Cu, Pd (left) and the positions of bond critical points (green balls) in the [Pd(acacen)] structure (right)

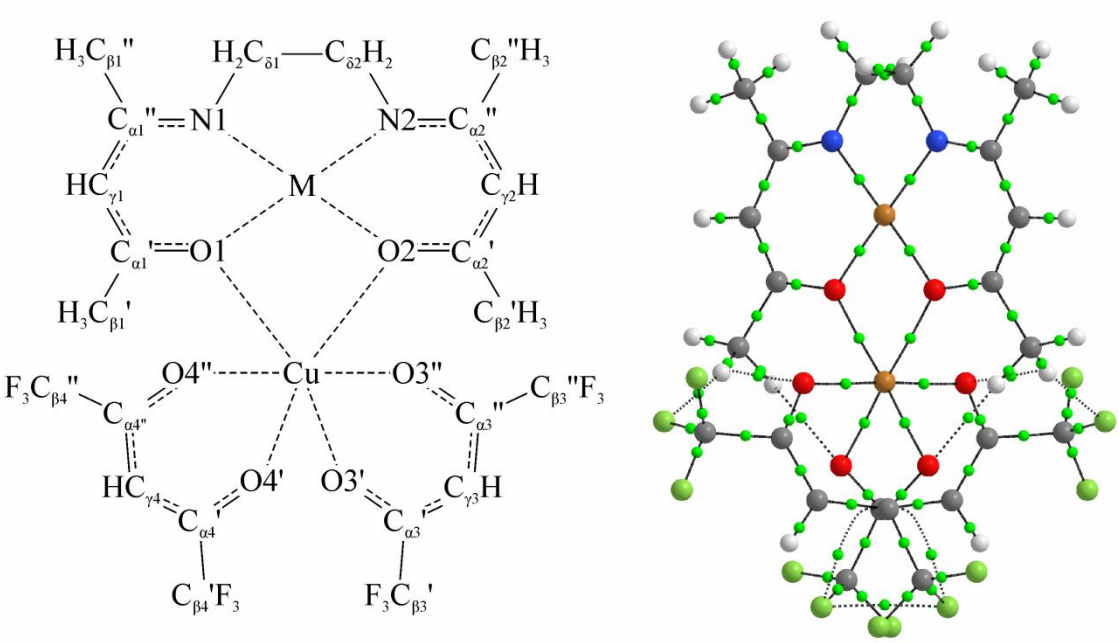

Figure 8. Structural formula of [M(acacen)Cu(hfac)$_2$], where M = Cu, Pd, (*left*); the positions of the bond critical points (green balls) in [Cu(acacen)Cu(hfac)$_2$] (*right*)